Novel Mono- and Di-ferrocenyl Bipyridyl Ligands: Syntheses, Electrochemistry, and Electropolymerisation Studies of their Ruthenium(II) Complexes

Paul D. Beer *,† **and Oldrich Kocian**
Department of Chemistry, University of Birmingham, P.O. Box 363, Birmingham B15 2TT
Roger J. Mortimer *
Department of Chemistry, University of Technology, Loughborough, Leicestershire LE11 3TU

The syntheses and electrochemical properties of new mono- and di-ferrocenyl bipyridyl ligands containing *trans* conjugated olefinic linkages between the ferrocene redox centres and the 4,4′-substituted 2,2′-bipyridine (bipy) moieties are described. The corresponding ruthenium(II) complexes have been prepared and one complex, $[RuL^4(bipy)_2][PF_6]_2$ [L^4 = 4,4′-bis(ferrocenylvinyl)-2,2′-bipyridine], undergoes electrochemical polymerisation to produce an electrochromic polymer film.

Interest in transition-metal polypyridyl complexes has grown rapidly in recent years due to their numerous applications in a variety of fields.[1] For example, 2,2′-bipyridine (bipy) complexes of ruthenium,[2,3] osmium,[4] and rhenium[5,6] exhibit properties of importance to redox electrocatalysis and solar-energy conversion.[7,8] With respect to the latter a currently active research field is the synthesis of chromophore-electroactive quencher systems in which electron-transfer acceptors (such as 4,4′-bipyridinium) and/or donors (such as phenothiazine) are covalently attached to $[Ru(bipy)_3]^{2+}$ species.[9] We report here the preparation, co-ordination, and electrochemical properties (including electropolymerisation studies) of novel 4,4′-disubstituted 2,2′-bipyridine ligands containing appended redox-active ferrocene electron-transfer donor moieties.

Results and Discussion

Syntheses of New Ligands.—Monolithiation of 4,4′-dimethyl-2,2′-bipyridine using 1.0 equivalent of lithium di-isopropylamide[10] in tetrahydrofuran (thf) followed by addition of ferrocenecarbaldehyde gave L^1 (77% yield, m.p. 129—130 °C) which on reaction with pyridinium toluene-*p*-sulphonate[11] afforded L^2 (95% yield, decomp. 160 °C), Scheme 1. Dilithiation of 4,4′-dimethyl-2,2′-bipyridine with 2.6 equivalents of $LiNPr^i_2$ and subsequent addition of ferrocenecarbaldehyde (2 mol) gave L^3 (55% yield, m.p. 180—181 °C). Dehydration of L^3 using pyridinium toluene-*p*-sulphonate gave L^4 (86% yield, decomp. 200 °C), Scheme 2. The structures of the new ferrocene–bipyridyl ligands were characterised by elemental analyses, mass spectrometry, and ^1H n.m.r. spectroscopy (see Experimental section). It is noteworthy that high-field ^1H n.m.r. spectroscopy suggests only the *trans* isomers of L^2 and L^4 were isolated.

Co-ordination Studies.—The monoligand ruthenium(II) complexes $[RuL^2(bipy)_2][PF_6]_2$ and $[RuL^4(bipy)_2][PF_6]_2$ were obtained by refluxing the appropriate ligand with $[RuCl_2(bipy)_2]\cdot 2H_2O$[12] in dimethylformamide (dmf), followed by addition of ammonium hexafluorophosphate. The electronic absorption spectra of these complexes were obtained in MeCN at concentrations of 5×10^{-4} mol dm^{-3} and the major absorption bands are reported in Table 1. The metal-to-ligand charge-transfer (m.l.c.t.) absorption bands appear at longer wavelengths in comparison to the value of 452 nm for the parent

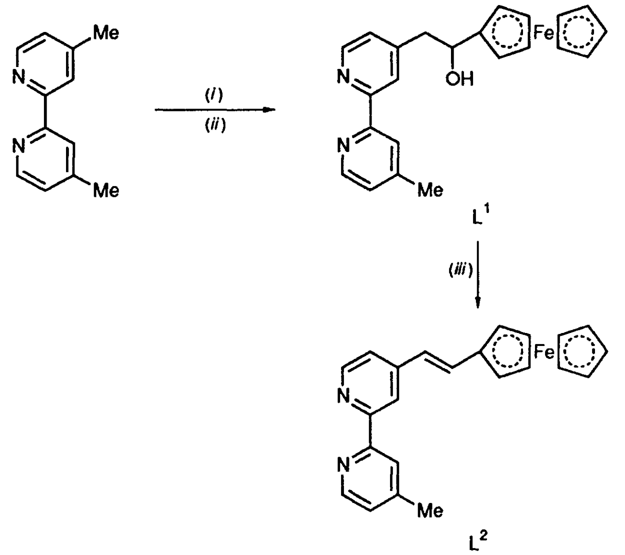

Scheme 1. (*i*) $LiNPr^i_2$; (*ii*) ferrocenecarbaldehyde; (*iii*) pyridinium toluene-*p*-sulphonate

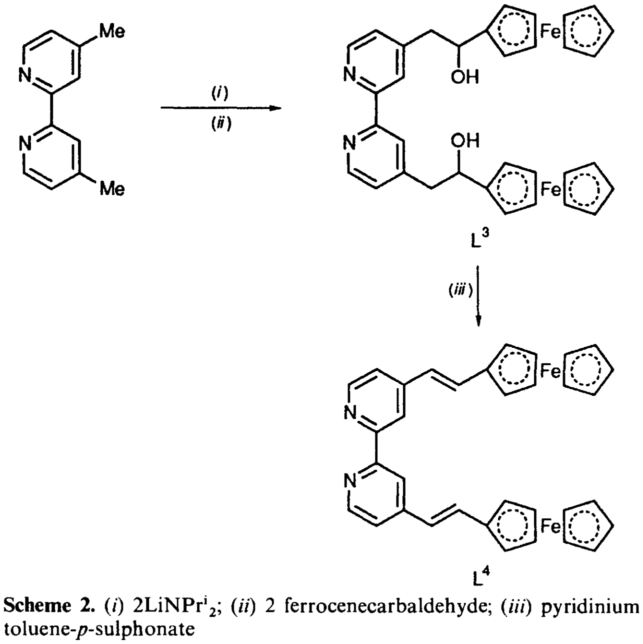

Scheme 2. (*i*) $2LiNPr^i_2$; (*ii*) 2 ferrocenecarbaldehyde; (*iii*) pyridinium toluene-*p*-sulphonate

---

† *Present address*: Inorganic Chemistry Laboratory, University of Oxford, South Parks Road, Oxford OX1 3QR.

Table 1. Electronic absorption data in (MeCN) for the ruthenium(II) complexes of L^2 and L^4

Complex	$\lambda_{max.}$/nm(ε/dm^3 mol^{-1} cm^{-1})
$[RuL^2(bipy)_2][PF_6]_2$	245 (30 400)
	289 (68 800)
	430 (11 700)
	456 (13 200)
$[RuL^4(bipy)_2][PF_6]_2$	244 (20 800)
	290 (45 600)
	432 (7 300)
	456 (8 300)
$[RuL^2_3][PF_6]_2$*	253
	300
	342
	540
$[RuL^4_3][PF_6]_2$	Insoluble

* Limited solubility.

Table 2. Electrochemical data for the ligands

Ligand	$E^{f\,a,b}$/V *vs.* s.c.e.	$\Delta E_p^{\,a,c}$/V
L^1	+0.45	0.10
L^3	+0.45	0.10
L^2	+0.52	0.10
L^4	+0.53	0.10
Ferrocene	+0.49	0.09

[a] Values quoted were (±0.01) at 200 mV s^{-1} in 3 × 10^{-3} mol dm^{-3} solutions of ligand in 0.2 mol dm^{-3} NBu_4BF_4–dmf. [b] $E_{p,c}$ = Cathodic peak potential, $E_{p,a}$ = anodic peak potential. Formal potential $E^f = \frac{1}{2}(E_{p,c} + E_{p,a})$. [c] Separation of peak potential $\Delta E_p = |E_{p,c} - E_{p,a}|$.

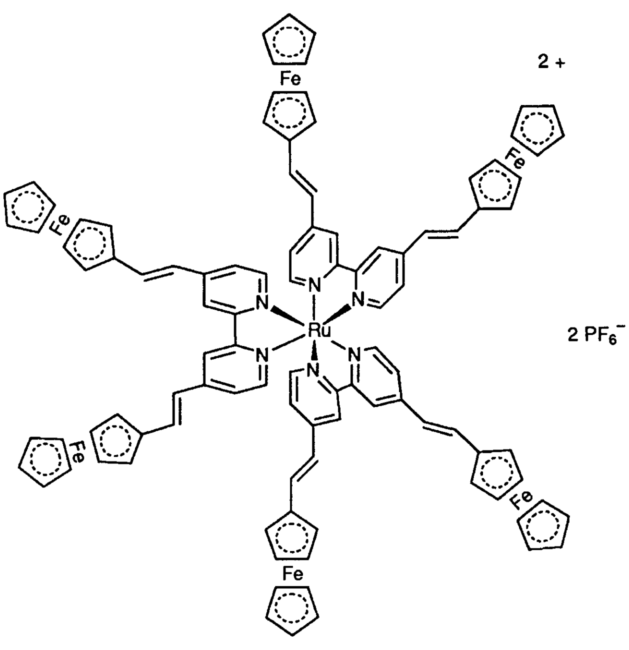

complex $[Ru(bipy)_3][PF_6]_2$. This is indicative of the electron-withdrawing nature of the respective olefinic ferrocenyl substituents, lowering the energy of the m.l.c.t. state.[13] The corresponding tris(ligand)ruthenium(II) complexes $[RuL^2_3][PF_6]_2$ and $[RuL^4_3][PF_6]_2$ (illustrated) were obtained by refluxing the appropriate ligand with $RuCl_3 \cdot 3H_2O$ in dmf, followed by addition of ammonium hexafluorophosphate. The major absorption bands for $[RuL^2_3][PF_6]_2$ are reported in Table 1. Unfortunately, $[RuL^4_3][PF_6]_2$ proved insoluble in all common solvents.

Electrochemical Studies of the New Ligands.—Table 2 shows formal potentials (E^f) and separations of peak potentials (ΔE_p) from the results of cyclic voltammetric experiments for the ligands in dmf. Ligands L^1 and L^2 each exhibit a quasi-reversible one-electron redox wave whereas L^3 and L^4 exhibit a single quasi-reversible two-electron redox wave, the number of electrons being confirmed by coulometry. The single-step redox processes of L^3 and L^4 indicate that the respective two ferrocene moieties do not electrochemically interact with one another either inductively through the conjugated system or through space. Comparison of E^f values for the ligands with that for ferrocene (Table 2) illustrates, the electron-withdrawing nature of the olefinic bond and the electron-donating nature of the alcohol linkage.

Electrochemical Studies of $[RuL^2(bipy)_2][PF_6]_2$.—Table 3 shows E^f and ΔE_p values for Ru^{III}–Ru^{II} ($E^f_{Ru^{III/II}}$), ferrocene ($E^f_{Fc^{+/0}}$) and the first two ligand-centred (E_1^f,E_2^f) redox waves in dmf and MeCN. The value of $E^f_{Fc^{+/0}}$ for ligand L^2 is unchanged on complexation with ruthenium(II) indicating that the metal centre does not exhibit a polarising effect on the ferrocene moiety. Likewise, $E^f_{Ru^{III/II}}$ for the complex is close to that for $[Ru(bipy)_3]^{2+}$,[14–16] showing that the ferrocene redox moiety exerts no stabilising effect. The E_1^f and E_2^f values for the complex are also close to those for $[Ru(bipy)_3]^{2+}$,[14–16] indicating correspondence to the reduction of the two bipy ligands. This is further supported by the observation that when a complex such as $[Ru(bipy)_2(mvbipy)]^{2+}$ (mvbipy = 4-methyl-4′-vinyl-2,2′-bipyridine) is electrochemically reduced by two electrons these electrons are largely (*ca.* 90%) localised on the two bipy ligands and not the mvbipy ligand.[17] Figure 1 illustrates that the third ligand-centred redox wave for reduction of L^2 in the complex is irreversible over the scan rate range of 10—100 mV s^{-1} and E^f, ΔE_p values are therefore not reported in Table 3.

Cathodic electropolymerisation reactions have been noted for a variety of tris(2,2′-bipyridyl) transition-metal complexes that have olefinic substituents on one or more ligands.[18] It was anticipated that sequential potential scanning of solutions of $[RuL^2(bipy)_2][PF_6]_2$ to the series of ligand-centred reductions would activate the olefinic linkage and initiate electropolymerisation. Currents for sequential potential scans at 100 mV s^{-1} were identical to that in Figure 1 indicating that polymer formation did not take place. Murray and co-workers[19] suggested that polymerisation of $[Ru(mvbipy)_3]^{2+}$ and related complexes proceeds by several pathways, the most important of which is a radical–radical coupling process. The complex $[RuL^2(bipy)_2][PF_6]_2$ contains only a single olefinic ligand and radical–radical coupling will result in dimeric products from a hydrodimerisation process. The broad pre-peak prior to the series of ligand-centred reductions and the irreversibility of the third reduction shows that product adsorption takes place. Figure 2, where the potential range is extended to include the ferrocene wave, indicates that the desorption process is slow. If the initial potential scan 0.00 to −1.90 V is followed by −1.90 to +0.80 V an enhanced oxidation current is observed that includes oxidation of the additional desorbed material. Restricting the potential range to the ferrocene redox wave restores the expected quasi-reversible process.

Electrochemical Studies of $[RuL^4(bipy)_2][PF_6]_2$.—Table 4 shows E^f and ΔE_p values for the ferrocene and the first two ligand-centred redox waves in dmf. The data again show that the redox moieties are independent. Likewise, Figure 3 illustrates that the third ligand-centred redox wave for reduction of L^4 in

Table 3. Electrochemical data for the ruthenium(II) complex of L^2

	2×10^{-3} mol dm^{-3} $[RuL^2(bipy)_2][PF_6]_2$–0.1 mol dm^{-3} NBu_4BF_4				$[Ru(bipy)_3]^{2\bullet}$	
	dmf		MeCN		dmf	MeCN
	$E^{f\,a}$/V *vs.* s.s.c.e.	$\Delta E_p{}^a$	$E^{f\,a}$/V *vs.* s.s.c.e.	$\Delta E_p{}^a$	E^f/V *vs.* s.c.e.	E^f/V *vs.* s.c.e.
$E^f{}_{Ru^{III/II}}$	*b*	*b*	+1.25	0.12	+1.24[c]	+1.32[d] +1.26[e]
$E^f{}_{Fc^{+/0}}$	+0.51	0.11	+0.40	0.10	—	—
$E^f{}_1$	−1.24	0.08	−1.34	0.11	−1.27[c]	−1.30[d] −1.35[e]
$E^f{}_2$	−1.42	0.12	−1.43	0.14	−1.46[c]	−1.49[d] −1.54[e]

[a] Values quoted were constant (±0.01) over the scan rate range utilised, 10—100 mV s^{-1}. [b] The Ru^{III}–Ru^{II} redox wave was not accessible in dmf. [c] Ref. 14. [d] Ref. 15. [e] Ref. 16.

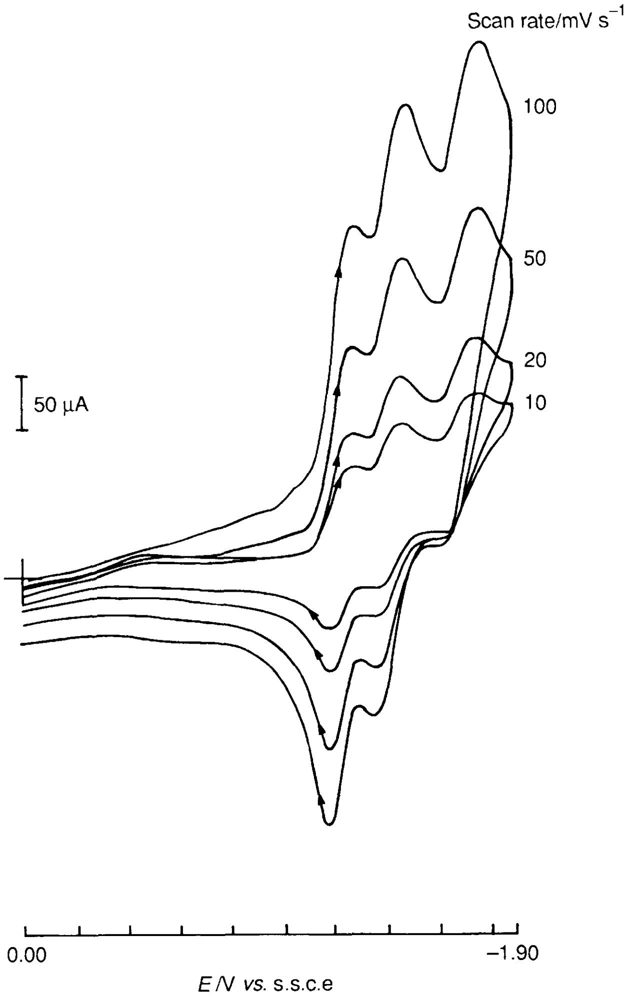

Figure 1. Cyclic voltammograms for a solution containing 2 mmol dm^{-3} $[RuL^2(bipy)_2][PF_6]_2$ in 0.1 mol dm^{-3} NBu_4BF_4–dmf as a function of scan rate

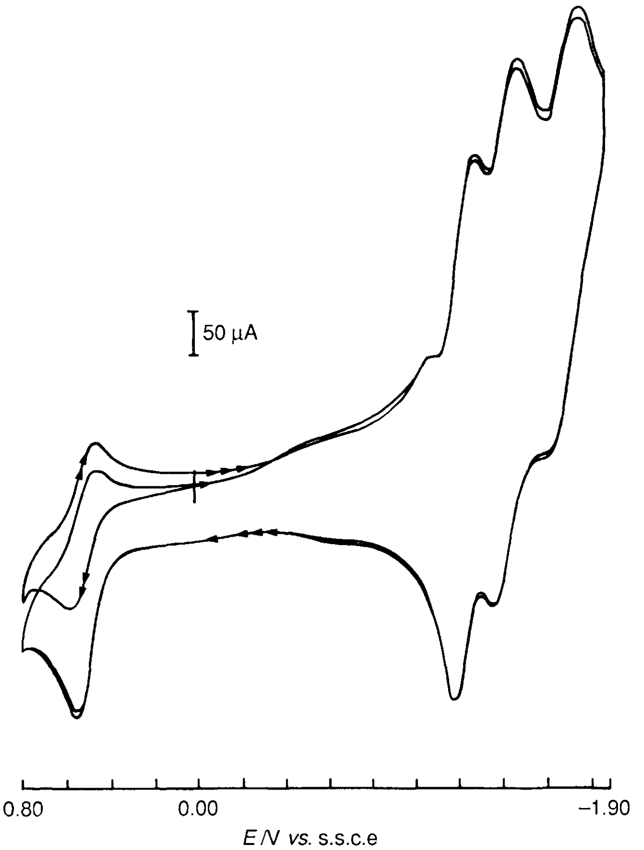

Figure 2. Three sequential cyclic voltammograms for a solution containing 2 mmol dm^{-3} $[RuL^2(bipy)_2][PF_6]_2$ in 0.1 mol dm^{-3} NBu_4BF_4–dmf at 100 mV s^{-1}. First scan (single arrow); 0.00 to −1.90 to +0.80 to 0.00 V. Second scan (double arrow): 0.00 to +0.80 to 0.00 V. Third scan (triple arrow): 0.00 to −1.90 to +0.80 to 0.00 V

Table 4. Electrochemical data for 1 × 10^{-3} mol dm^{-3} $[RuL^4(bipy)_2][PF_6]_2{}^a$–0.1 mol dm^{-3} NBu_4BF_4 in dmf

	$E^{f\,b}$/V *vs.* s.s.c.e.	$\Delta E_p{}^b$/V
$E^f{}_{Fc^{+/0}}$	+0.50	0.10
$E^f{}_1$	−1.22	0.08
$E^f{}_2$	−1.40	0.08

[a] The complex has limited solubility in dmf; maximum concentration achieved = 1 × 10^{-3} mol dm^{-3} [b] Values quoted were constant (±0.01) over the scan rate range utilised, 10—100 mV s^{-1}.

the complex is irreversible over the scan rate range of 10—100 mV s^{-1} and E^f, ΔE_p values are therefore not reported in Table 4.

Sequential potential scans of solutions of the complex to the series of ligand-centred reductions again did not initiate electropolymerisation. Figures 3 and 4 show voltammetric features for adsorption/desorption comparable to those in Figures 1 and 2. Sequential potential scanning to include the metal-centred Ru^{III}–Ru^{II} and ferrocene redox waves (both accessible in

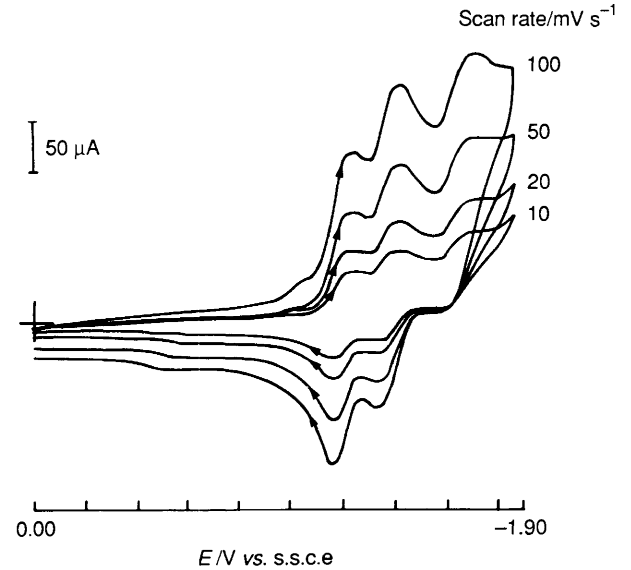

Figure 3. Cyclic voltammograms for a solution containing 1 mmol dm^{-3} [RuL^4(bipy)$_2$][PF$_6$]$_2$ in 0.1 mol dm^{-3} NBu$_4$BF$_4$–dmf as a function of scan rate

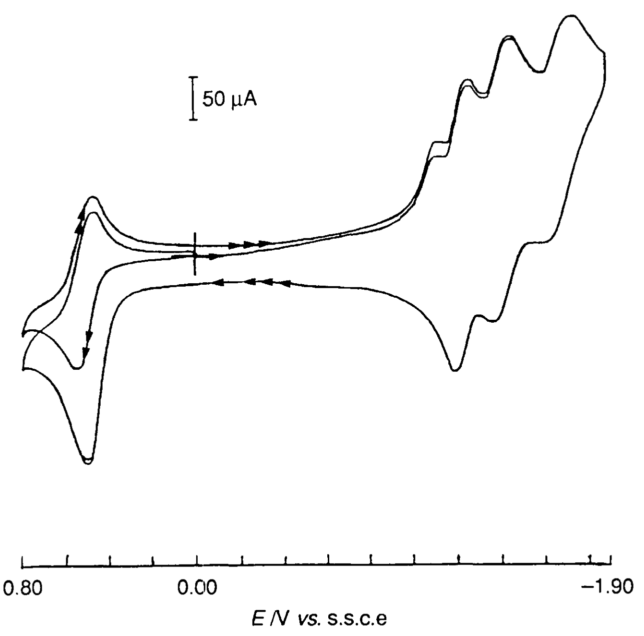

Figure 4. Three sequential cyclic voltammograms for a solution containing 2 mmol dm^{-3} [RuL^4(bipy)$_2$][PF$_6$]$_2$ in 0.1 mol dm^{-3} NBu$_4$BF$_4$–dmf at 100 mV s^{-1}. Potential programme as for Figure 2

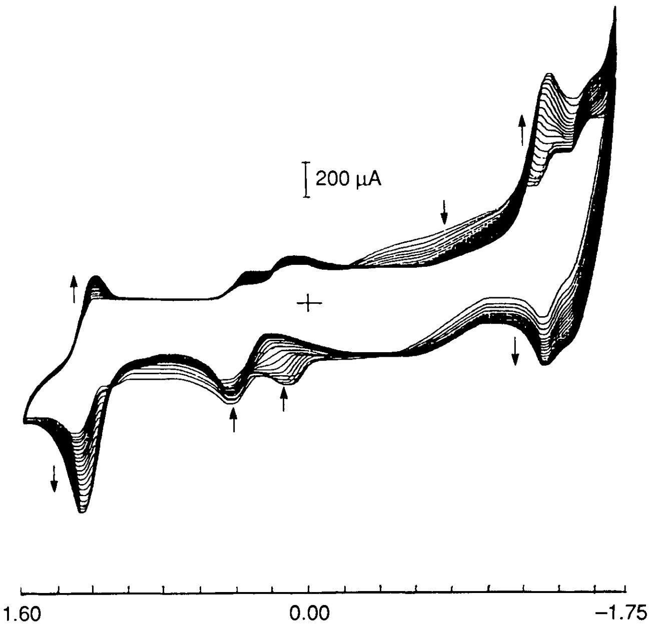

Figure 5. Twenty sequential cyclic voltammograms for a solution containing 1 mmol dm^{-3} [RuL^4(bipy)$_2$][PF$_6$]$_2$ in 0.1 mol dm^{-3} NBu$_4$BF$_4$–MeCN at 100 mV s^{-1}. Potential programme 0.00 to −1.75 to +1.60 to 0.00 V. The vertical arrows indicate current increase or decrease as appropriate

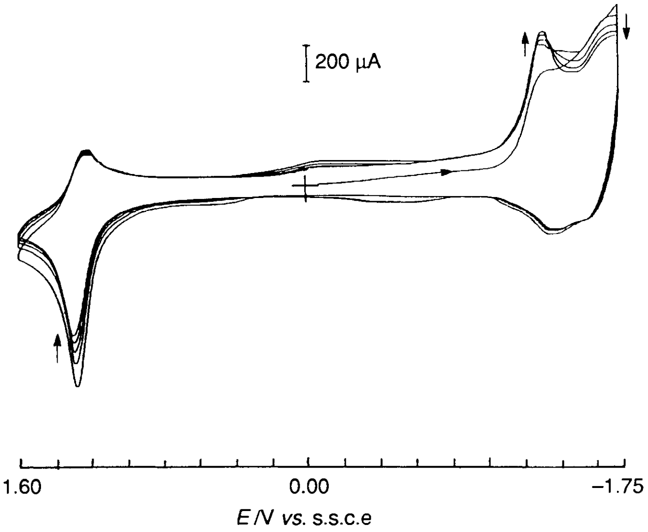

Figure 6. Five sequential cyclic voltammograms for the poly-[RuL^4(bipy)$_2$]$^{2+}$ modified electrode from Figure 5 in 0.1 mol dm^{-3} NBu$_4$BF$_4$–MeCN at 100 mV s^{-1}. Potential programme as for Figure 5

MeCN) did however cause polymer film formation. Figure 5 shows the steady increase in current attributable to the combined electroactivity of the polymeric film and that of the inward-diffusing complex. On removal of the electrode a smooth, adherent, golden-yellow film is observed. Figure 6 shows sequential cyclic voltammograms of such a poly-[RuL^4(bipy)$_2$]$^{2+}$ modified electrode in complex-free supporting electrolyte. Current is revealed for the Ru^{III}–Ru^{II} and ligand-centred redox processes. The ferrocene redox process is absent, suggesting either that the ferrocene is electroinactive in the polymer or partial decomposition of the complex in the electropolymerisation. Interestingly, the polymer film was electrochromic changing from golden yellow to transparent on full oxidation to the ruthenium(III) redox state. Plots of log(peak current) for the Ru^{III}–Ru^{II} redox wave ($E^f = +1.25$ V) *versus* log(scan rate) over the range 10—200 mV s^{-1} had a slope of 0.65 indicating a combination of diffusional (expected slope 0.50) and surface-attached (expected slope 1.00) polymer film behaviour.

Conclusion

These preliminary studies indicate that careful design of ferrocene-linked 2,2′-bipyridine ruthenium complexes is necessary for preparation of polymeric films that contain chromophore-electroactive quencher systems. Earlier studies by Murray and co-workers[18] with the related transition-metal complexes of 4,4′-distyryl-2,2′-bipyridine and 4,4′-bis(*p*-methylstyryl-2,2′-bipyridine) ligands showed that complexes containing greater numbers of these ligands undergo electropolymerisation more rapidly. Thus in the present study the tris complexes would be expected to show the highest electropolymerisation rate. Electrochemical measurements however are precluded due to the insolubility of the respective $[RuL^2{}_3][PF_6]_2$ and $[RuL^4{}_3][PF_6]_2$ complexes. In contrast $[RuL^2(bipy)_2][PF_6]_2$ with only a single olefinic ligand did not electropolymerise, showing the importance of radical–radical coupling; $[RuL^4(bipy)_2][PF_6]_2$ with two olefinic groups on ligand L^4 successfully electropolymerised, but only if the potential range included the oxidation reactions. It seems likely that the oxidative reactions include precipitation of the oligomers that are formed on the reduction scan. The necessity of the oxidation scan for successful polymer film formation was not needed for the analogous complex of 4,4′-distyryl-2,2′-bipyridine suggesting that linkage through the phenyl group is important in polymer formation.

Experimental

Proton n.m.r. spectra were recorded on a JEOL GX 270 spectrometer at 270.05 MHz at 20 °C using tetramethylsilane as the internal reference, i.r. spectra as KBr pellets on a Perkin-Elmer 297 spectrophotometer over the range 4 000—600 cm^{-1}, and electronic absorption spectra on a Perkin-Elmer 330 spectrophotometer in MeCN. Electron-impact (70 eV, *ca.* 1.12×10^{-17} J) and fast atom bombardment (f.a.b) mass spectra (matrix: *m*-nitrobenzyl alcohol) were taken on a Kratos MS80 RF mass spectrometer with a DS90 data system. Microanalyses were performed on a Perkin-Elmer Model 1201 automatic analyser. Electrochemical studies were performed using Princeton Applied Research instrumentation. A three-electrode system was employed with platinum bead (for Table 2 data) or 1-cm^2 platinum flag (for the remainder of the measurements) working electrodes. The reference electrode was either a saturated calomel electrode (s.c.e.) (for Table 2 data) or a sodium chloride saturated calomel electrode (s.s.c.e.) (for the remainder of the measurements) with a platinum-mesh counter electrode. Measurements were carried out in MeCN and dmf containing 0.2 (for Table 2 data) or 0.1 mol dm^{-3} (for the remainder of the measurements) tetrabutylammonium tetrafluoroborate as supporting electrolyte.

Analytical samples were dried *in vacuo* (6.5 Pa) at 65 °C. Melting points, uncorrected, were taken in glass capillary tubes on a Gallenkamp melting apparatus.

Thin-layer chromatography was carried out on Merck Kieselgel $60F_{254}$ precoated silica gel plates. Preparative flash chromatography was performed either on basic Merck TLC alumina of 60 H (type E) or TLC-Kieselgel 60 H with the solvent specified.

Materials.—4,4′-Dimethyl-2,2′-bipyridine, ferrocenecarbaldehyde, *n*-butyl-lithium in hexane, and ruthenium(III) chloride trihydrate were commercial products (Aldrich); $[RuCl_2(bipy)_2]\cdot 2H_2O$[12] and pyridinium toluene-*p*-sulphonate[11] were prepared by described procedures.

Tetrahydrofuran and toluene were distilled from sodium diphenylketyl, di-isopropylamine and acetonitrile from calcium hydride prior to use. Dimethylformamide was distilled from P_2O_5 under reduced pressure and stirred over 4-Å molecular sieves. All other solvents employed were of reagent grade.

Synthesis of the Ligands.—*4-[2-(Ferrocenyl)-2-hydroxyethyl]-4′-methyl-2,2′-bipyridine* (L^1). A three-necked flask (500 cm^3) equipped with magnetic stirrer, thermometer, pressure-equalising dropping funnel, and side arm connected to a nitrogen bubbler system was charged with di-isopropylamine (4.0 cm^3, 28.5 mmol) and dry thf (30.0 cm^3). The flask was flushed with nitrogen, and a slight positive pressure was maintained with a slow stream of nitrogen. The solution was cooled to about −75 °C with an acetone–solid CO_2 bath and 1.6 mol dm^{-3} n-butyl-lithium (17.5 cm^3, 28.0 mmol) in hexane was added. The pale yellow solution was stirred at −75 °C for 30 min and then a solution of 4,4′-dimethyl-2,2′-bipyridine (5.0 g, 27.0 mmol) in dry thf (150 cm^3) was added *via* a dropping funnel to produce a dark brown-red solution.

The acetone-solid CO_2 bath was replaced with an ice–water bath, and the mixture was stirred at 0 °C for 1 h. To the cold solution was added ferrocenecarbaldehyde (6.4 g, 30.0 mmol) in thf (30 cm^3) in one portion *via* a syringe. Stirring was continued at 0 °C for 1 h and then at room temperature for 3 h. The mixture was quenched with methanol (3 cm^3), poured into water, and extracted with several portions of chloroform. The combined extracts were washed with brine, dried over $MgSO_4$, and the solvent removed *in vacuo*. The residue was subjected to flash chromatography on silica gel using CH_2Cl_2–MeOH–aqueous NH_4OH (100:2:0.5) giving L^1 (8.3 g, 77%), m.p. 129—130 °C (decomp.). U.v. (MeCN): $\lambda_{max.}(\varepsilon)$ 280 (17 800) and 242 nm (17 000 dm^3 mol^{-1} cm^{-1}). I.r. (KBr): 3 250, 3 075, 2 850, 1 600, 1 550, 1 460, 1 370, and 1 070 cm^{-1}. ^1H N.m.r. ($CDCl_3$): δ 2.19 (d, 1 H, *J* = 3.1, OH), 2.44 (s, 3 H, CH_3), 3.02 (d, 2 H, *J* = 6.6 Hz, CH_2), 4.12—4.27 (m, 9 H, ferrocene H), 4.66—4.72 (m, 1 H, CHOH), 7.12—7.14 (m, 2 H, $H^{5,5'}$ of bipy), 8.23 (s, 1 H, $H^{3'}$ of bipy), 8.28 (s, 1 H, H^3 of bipy), and 8.53—8.57 (m, 2 H, $H^{6,6'}$ of bipy). Mass spectrum: *m/z* (relative intensity) 398 (4, M^+), 380 (67), 315 (100), 303 (30), 257 (10), 214 (10), 184 (26) and 121 (9) (Found for semihydrate: C, 68.1; H, 5.4; N, 6.9. Calc. for $C_{23}H_{22}FeN_2O$: C, 69.35; H, 5.55; N, 7.05%).

4,4′-Bis[2-ferrocenyl-2-hydroxyethyl]-2,2′-bipyridine (L^3).—A three-neck flask (500 cm^3), equipped with a magnetic stirrer, thermometer, pressure-equalising dropping funnel, and side arm connected to a nitrogen bubbler system, was charged with di-isopropylamine (7.5 cm^3, 53.5 mmol) and dry thf (40.0 cm^3). The flask was flushed with nitrogen, and a slight positive pressure was maintained with a slow stream of nitrogen. The solution was cooled to about −75 °C with an acetone–solid CO_2 bath and 1.6 mol dm^{-3} n-butyl-lithium (33.0 cm^3, 52.8 mmol) in hexane was added. The pale yellow solution was stirred at −70 °C for 30 min and a solution of 4,4′-dimethyl-2,2-bipyridine (3.9 g, 21.2 mmol) in dry thf (120 cm^3) was added *via* a dropping funnel to produce a dark orange-red solution. The acetone–solid CO_2 bath was replaced with an ice–water bath, and the mixture was stirred at 0 °C for 1 h before ferrocenecarbaldehyde (9.1 g, 42.5 mmol) in dry thf (30 cm^3) was added *via* a syringe. Stirring was maintained at 0 °C for 1 h and then at room temperature for 5 h. The mixture was quenched with methanol (3 cm^3), poured into water (200 cm^3), and extracted with $CHCl_3$ (3 × 100 cm^3). The combined extracts were washed with brine, dried over $MgSO_4$, and the solvent removed *in vacuo*. Additions of acetone to the residue gave the pure product as a yellow solid (4.1 g), m.p. 180—181 °C. The acetone mother-liquors were evaporated and the residue was subjected to flash chromatography on alumina with 2% MeOH–CH_2Cl_2, giving a second crop of L^3 (3.0 g) and bringing the total yield to 7.1 g (55%). U.v. (MeCN): $\lambda_{max.}(\varepsilon)$ 278 (3 360) and 240 nm (3 680 dm^3 mol^{-1} cm^{-1}). I.r. (KBr): 3 300, 3 070, 1 600, 1 550, 1 460, 1 380, and 1 050 cm^{-1}. ^1H N.m.r. [$(CD_3)_2SO$]: δ 2.92—2.96 (m, 2 H, CH_2), 3.11—3.16 (m, 2 H, CH_2), 4.11—4.26 (m, 18 H, ferrocene H), 4.64 (m, 2 H, CHOH), 4.93 (d, 2 H, *J* = 6.2, OH), 7.34 (d, 2 H, *J* = 3.5, $H^{5,5'}$ of bipy), 8.34 (s, 2 H, $H^{3,3'}$ of bipy), and 8.57 (d, 2 H, *J* = 4.9 Hz, $H^{6,6'}$ of bipy). F.a.b. Mass spectrum: *m/z* (relative intensity) 612 (100, M^+), 595 (18), 519

(15), 457 (45), 409 (237), 397 (29), 361 (15), 332 (21), 314 (279), 215 (36), and 186 (78) (Found: C, 66.6; H, 5.4; N, 4.6. Calc. for $C_{34}H_{32}Fe_2N_2O_2$: C, 66.7; H, 5.25; N, 4.55%).

Synthesis of the (E)-*Alkenes* (L^2) *and* (L^4).—A mixture of the appropriate alcohol (5.0 mmol), pyridinium toluene-*p*-sulphonate[11] (1.2 mmol), and dry toluene (160 cm^3) was stirred under reflux with removal of water for 5 h, then cooled to room temperature and the toluene removed *in vacuo*. The residue was dissolved in $CHCl_3$ and successively washed with water, brine, then dried ($MgSO_4$). The solvent was removed *in vacuo* to give the crude product which was column-chromatographed on alumina using chloroform–methanol as eluant to give the corresponding product.

4-*Ferrocenylvinyl*-4′-*methyl*-2,2′-*bipyridine* (L^2): yield 95%, m.p. decomp. ≈ 160 °C. U.v. (MeCN): $\lambda_{max.}(\varepsilon)$ 252 (25 400), 310 (26 400), 376 (3 660), and 470nm (2 120 $dm^3\ mol^{-1}\ cm^{-1}$). I.r. (KBr): 1 625, 1 590, 1 540, 1 450, 1 365, 1 100, and 960 cm^{-1}.

^1H N.m.r. ($CDCl_3$): δ 2.45 (s, 3 H, CH_3), 4.15 (s, 5 H, ferrocene H), 4.35 (t, 2 H, J = 1.6, ferrocene H), 4.51 (t, 2 H, J = 1.8, ferrocene H), 6.71 (d, 1 H, J = 16.1, =CH–), 7.15 (d, 1 H, J = 3.9, H^5 of bipy), 7.20—7.26 (m, 1 H, $H^{5'}$ of bipy), 7.28 (d, 1 H, J = 16.0 Hz, =CH–), 8.26 (s, 1 H, H^3 of bipy), 8.44 (s, 1 H, $H^{3'}$ of bipy), and 8.57—8.60 (m, 2 H, $H^{6,6'}$ of bipy). Mass spectrum: m/z (relative intensity) 380 (36, M^+), 315 (54), 310 (16), 257 (5), 184 (12), 91 (100), and 65 (8) (Found: C, 72.3; H, 5.6; N, 7.2. Calc. for $C_{23}H_{20}FeN_2$: C, 72.65; H, 5.30; N, 7.35%).

4,4′-*Bis(ferrocenylvinyl)*-2,2′-*bipyridine* (L^4): yield 86%, m.p. decomp. ≈ 200 °C, (crystallised from CH_2Cl_2–MeOH). U.v.–visible (MeCN): $\lambda_{max.}$: 255, 316, 376, and 470 nm. I.r. (KBr): 1 625, 1 590, 1 540, 1 450, 1 100, and 960 cm^{-1}. ^1H N.m.r. ($CDCl_3$): δ 4.17 (s, 10 H, ferrocene H), 4.37 (s, 4 H, ferrocene H), 4.53 (s, 4 H, ferrocene H), 6.73 (d, 2 H, J = 16.1, =CH–), 7.26–7.32 (m, 4 H, $H^{5,5'}$ of bipy and =CH–), 8.46 (s, 2 H, $H^{3,3'}$ of bipy), and 8.63 (d, 2 H, J = 4.8 Hz, $H^{6,6'}$ of bipy) (Found for 1.5 CH_2Cl_2 solvate: C, 70.3; H, 4.6; N, 4.3. Calc. for $C_{34}H_{28}Fe_2N_2$: C, 70.85; H, 4.90; N, 4.85%).

Preparation of $[RuL(bipy)_2][PF_6]_2$ (L = L^2 *or* L^4).—A mixture of $[RuCl_2(bipy)_2]\cdot 2H_2O$[1] (260 mg, 0.5 mmol) and the appropriate ligand (0.5 mmol) in dry dmf (20 cm^3) was stirred and heated to reflux under nitrogen for 24 h. The solution was cooled to room temperature, then filtered, treated with ammonium hexafluorophosphate (0.4 g, 2.5 mmol) dissolved in water (5 cm^3), and left to stand at 0 °C for 3 h. The resultant dark precipitate was collected on a frit, washed separately with water, and dried *in vacuo* (silica gel).

Bis(2,2′-bipyridine)(4-ferrocenylvinyl-4′-methyl-2,2′-bipyridine)ruthenium(II) hexafluorophosphate $[RuL^2(bipy)_2][PF_6]_2$: yield 83%, dark brown solid. I.r. (KBr): 3 620, 3 400, 3 075, 1 620, 1 600, 1 460, 1 440, 1 420, and 840 cm^{-1} (Found: C, 46.2; H, 3.7; N, 7.8. Calc. for $C_{43}H_{36}F_{12}FeN_6P_2Ru\cdot 2H_2O$: C, 46.1; H, 3.60; N, 7.5%).

Bis(2,2′-bipyridine)[4,4′-bis(ferrocenylvinyl)-2,2′-bipyridine] ruthenium(II) hexafluorophosphate $[RuL^4(bipy)_2][PF_6]_2$: yield 73.5%, dark brown solid. I.r. (KBr): 3 400, 3 075, 1 620, 1 600, 1 460, 1 440, 1 420, and 840 cm^{-1} (Found: C, 49.3; H, 3.5; N, 6.1. Calc. for $C_{54}H_{44}F_{12}Fe_2N_6P_2Ru\cdot 2H_2O$: C, 49.3; H, 3.7; N, 6.4%).

Preparation of $[RuL_3][PF_6]_2$ (L = L^2 *or* L^4).—To a solution of $RuCl_3\cdot 3H_2O$ (66 mg, 0.25 mmol) in dry dmf (10 cm^3) was added the appropriate ligand (1.0 mmol), and the mixture was refluxed under nitrogen for 27 h. The solution was cooled to room temperature and filtered to remove the excess of the ligand. Addition of excess of aqueous NH_4PF_6 (10.3 g per 5 cm^3) led to precipitation of a black solid. The solid was collected by suction filtration, repeatedly washed with water, and dried *in vacuo* (silica gel).

Tris(ferrocenylvinyl-4′-methyl-2,2′-bipyridine)ruthenium(II) hexafluorophosphate $[RuL^2{}_3][PF_6]_2$: Yield 84%, black-red solid with limited solubility in MeCN and dmf. I.r. (KBr): 3 620, 3 400, 3 075, 2 920, 1 600, 1 480, 1 420, 1 020, and 840 cm^{-1} (Found: C, 52.1; H, 4.1; N, 5.2. Calc. for $C_{69}H_{60}F_{12}Fe_3N_6P_2Ru\cdot 3H_2O$: C, 52.25; H, 4.20; N, 5.3%).

Tris[4,4′-bis(ferrocenylvinyl)-2,2′-bipyridine]ruthenium(II) hexafluorophosphate $[RuL^4{}_3][PF_6]_2$: yield 72%, black solid almost insoluble in MeCN, dmf, Me_2SO, toluene, methanol, acetone, and CH_2Cl_2. I.r. (KBr): 3 400, 3 075, 2 920, 1 600, 1 480, 1 420, 1 010, and 840 cm^{-1} (Found: C, 56.4; H, 4.2; N, 3.7. Calc. for $C_{102}H_{84}F_{12}Fe_6N_6P_2Ru\cdot 3H_2O$: C, 56.35; H, 4.15; N, 3.85%).

Acknowledgements

We thank the S.E.R.C. for a postdoctoral research fellowship (to O. K.) and for use of the high-field n.m.r. service at the University of Warwick and the mass spectrometry service at University College Swansea. P. D. B. acknowledges additional financial support from Research Corporation Trust, L. and D. Blond, and R. J. M. acknowledges a Nuffield Foundation Grant.

References

1 C. Creutz, *Comments Inorg. Chem.*, 1982, **1**, 293.
2 E. A. Seddon and K. R. Seddon, 'The Chemistry of Ruthenium,' Elsevier, Amsterdam, 1984.
3 A. Juris, F. Barigelletti, S. Campagna, V. Balzani, P. Belser, and A. von Zeleswsky, *Coord. Chem. Rev.*, 1988, **84**, 85.
4 M. E. Kober, J. V. Caspar, R. S. Lumpkin, and T. J. Meyer, *J. Phys. Chem.*, 1986, **90**, 3722.
5 J. V. Caspar and T. J. Meyer, *J. Phys. Chem.*, 1983, **87**, 952.
6 A. Juris, S. Campagna, I. Bidd, J. M. Lehn, and R. Ziessel, *Inorg. Chem.*, 1988, **27**, 4007.
7 T. J. Meyer, *Acc. Chem. Res.*, 1989, **22**, 163.
8 J. S. Connolly, 'Photochemical Conversion and Storage of Solar Energy,' Academic Press, New York, 1981.
9 E. Danielson, C. M. Elliott, J. W. Merkert, and T. J. Meyer, *J. Am. Chem. Soc.*, 1987, **109**, 2519.
10 P. K. Ghosh and T. G. Spiro, *J. Am. Chem. Soc.*, 1980, **102**, 5543.
11 M. Miyashita, A. Yoshikoshi, and P. A. Grieco, *J. Org. Chem.*, 1977, **42**, 3372.
12 P. A. Lay, A. M. Sargeson, and H. Taube, *Inorg. Synth.*, 1986, **24**, 291.
13 R. P. Thummel, V. Hegole, and Y. Jahng, *Inorg. Chem.*, 1989, **28**, 3264.
14 C. M. Elliott and E. J. Hersheuhart, *J. Am. Chem. Soc.*, 1982, **104**, 7519.
15 N. E. Tokel-Takvoryan, R. W. Hemingway, and A. J. Bard, *J. Am. Chem. Soc.*, 1973, **95**, 6582.
16 F. Barigelletti, L. DeCola, V. Balzani, P. Belser, A. von Zelewsky, F. Vögtle, F. Ebmeyer, and S. Grammenudi, *J. Am. Chem. Soc.*, 1989, **111**, 4662.
17 C. M. Elliott, C. J. Baldy, L. M. Nuwaysir, and C. L. Wilkins, *Inorg. Chem.*, 1990, **29**, 389.
18 C. R. Leidner, B. P. Sullivan, R. A. Reed, B. A. White, M. T. Grimmins, R. W. Murray, and T. J. Meyer, *Inorg. Chem.*, 1987, **26**, 882 and refs. therein.
19 J. M. Calvert, R. H. Schmehl, B. P. Sullivan, J. S. Facci, T. J. Meyer, and R. W. Murray, *Inorg. Chem.*, 1983, **22**, 2151.

Received 30*th March* 1990; *Paper* 0/01384F